

Precise Measurement of the D_s^\pm Meson Lifetime

P. L. Frabetti,¹ H. W. K. Cheung,² J. P. Cumalat,² C. Dallapiccola,² J. F. Ginkel,² S. V. Greene,² W. E. Johns,² M. S. Nehrung,² J. N. Butler,³ S. Cihangir,³ I. Gaines,³ P. H. Garbincius,³ L. Garren,³ S. A. Gourlay,³ D. J. Harding,³ P. Kasper,³ A. Kreymer,³ P. Lebrun,³ S. Shukla,³ S. Bianco,⁴ F. L. Fabbri,⁴ S. Sarwar,⁴ A. Zallo,⁴ R. Culbertson,⁵ R. W. Gardner,⁵ R. Greene,⁵ J. Wiss,⁵ G. Alimonti,⁶ G. Bellini,⁶ B. Caccianiga,⁶ L. Cinquini,⁶ M. Di Corato,⁶ M. Giammarchi,⁶ P. Inzani,⁶ F. Leveraro,⁶ S. Malvezzi,⁶ D. Menasce,⁶ E. Meroni,⁶ L. Moroni,⁶ D. Pedrini,⁶ L. Perasso,⁶ A. Sala,⁶ S. Sala,⁶ D. Torretta,^{6,*} M. Vittone,^{6,*} D. Buchholz,⁷ D. Claes,⁷ B. Gobbi,⁷ B. O'Reilly,⁷ J. M. Bishop,⁸ N. M. Cason,⁸ C. J. Kennedy,⁸ G. N. Kim,⁸ T. F. Lin,⁸ D. L. Pušeljčić,⁸ R. C. Ruchti,⁸ W. D. Shephard,⁸ J. A. Swiatek,⁸ Z. Y. Wu,⁸ V. Arena,⁹ G. Boca,⁹ C. Castoldi,⁹ R. Diaferia,^{9,†} G. Gianini,⁹ S. P. Ratti,⁹ C. Riccardi,⁹ P. Vitulo,⁹ A. Lopez,¹⁰ G. P. Grim,¹¹ V. S. Paolone,¹¹ P. M. Yager,¹¹ J. R. Wilson,¹² P. D. Sheldon,¹³ F. Davenport,¹⁴ J. F. Filasetta,¹⁵ G. R. Blackett,¹⁶ M. Pisharody,¹⁶ T. Handler,¹⁶ B. G. Cheon,¹⁷ J. S. Kang,¹⁷ and K. Y. Kim¹⁷

(E687 Collaboration)

¹*Dipartimento di Fisica dell'Università and Istituto Nazionale di Fisica Nucleare-Bologna, I-40126 Bologna, Italy*

²*University of Colorado, Boulder, Colorado 80309*

³*Fermilab, Batavia, Illinois 60510*

⁴*Laboratori Nazionali di Frascati dell'Istituto Nazionale di Fisica Nucleare, I-00044 Frascati, Italy*

⁵*University of Illinois at Urbana-Champaign, Urbana, Illinois 61801*

⁶*Dipartimento di Fisica dell'Università and Istituto Nazionale di Fisica Nucleare-Milano, I-20133 Milano, Italy*

⁷*Northwestern University, Evanston, Illinois 60208*

⁸*University of Notre Dame, Notre Dame, Indiana 46556*

⁹*Dipartimento di Fisica Nucleare e Teorica dell'Università and Istituto Nazionale di Fisica Nucleare-Pavia, I-27100 Pavia, Italy*

¹⁰*University of Puerto Rico at Mayaguez, Puerto Rico*

¹¹*University of California-Davis, Davis, California 95616*

¹²*University of South Carolina, Columbia, South Carolina 29208*

¹³*Vanderbilt University, Nashville, Tennessee 37235*

¹⁴*University of North Carolina-Asheville, Asheville, North Carolina 28804*

¹⁵*Northern Kentucky University, Highland Heights, Kentucky 41076*

¹⁶*University of Tennessee, Knoxville, Tennessee 37996*

¹⁷*Korea University, Seoul 136-701, Korea*

(Received 23 February 1993)

A precise measurement of the D_s^\pm meson lifetime is reported. The data were accumulated by the high energy photoproduction experiment E687 at Fermilab in the 1990–1991 fixed target run. The measurement has been done using 900 fully reconstructed $D_s^\pm \rightarrow \phi\pi^\pm$ decays. The lifetime of the D_s^\pm meson is measured to be $0.475 \pm 0.020 \pm 0.007$ ps.

PACS numbers: 14.40.Jz, 13.25.+m

The lifetime of the D_s meson has not been measured as precisely as the lifetimes of the D^0 and the D^+ mesons primarily because of its lower production rate. (States and their charge conjugates are implied in this paper except where otherwise explicitly stated.) The accuracy of recent measurements [1–4] of the D_s lifetime is such that the average lifetime is consistent with being equal to that of the D^0 meson (at about the 10% level), while it is shorter than that of the D^+ meson by more than a factor of 2. Although the D_s and the D^0 are expected to have equal lifetimes in the naive spectator model, differences are expected when more realistic calculations are carried out which take into account interference, weak annihilation, τ decay modes, and relativistic effects. A more precise measurement of the D_s meson lifetime is

needed in order to constrain calculations taking these effects into account. This paper reports a new precise measurement of the D_s meson lifetime based on 900 fully reconstructed decays to the $\phi\pi^\pm$ final state from a sample of about 5×10^8 hadronic triggers obtained with the Fermilab wide band photon spectrometer.

The E687 detector [5] is a large aperture multiparticle magnetic spectrometer with excellent vertex measurement, particle identification, and calorimetric capabilities. This experiment used a high energy bremsstrahlung photon beam and a Be target. The average tagged photon momentum was 220 GeV/c. Charged particles coming from the Be target were tracked by twelve planes of silicon microstrips providing high resolution tracking in the vertex region. The average resolution in the sepa-

ration between primary and secondary vertices for D_s decays obtained with this detector was $650 \mu\text{m}$, corresponding to an average proper time resolution of 0.05 ps . Following the microstrip system, charged particles passed through two analysis magnets interleaved with five stations of multiwire proportional chambers (PWCs). Three multicell threshold Čerenkov counters allowed kaon-pion separation over the momentum range from 4.5 to $61.5 \text{ GeV}/c$. The experimental trigger required that at least two charged tracks be present in the spectrometer outside the Bethe-Heitler pair region and that energy deposited in the hadronic calorimeter be greater than 40 GeV .

The initial data sample was obtained by selecting ϕ candidates identified by the decay $\phi \rightarrow K^+K^-$. Each of the decay secondaries was required to form an acceptable track in both the microstrip and multiwire proportional chamber systems; the two sets of parameters for a track had to be consistent within measurement errors. A ϕ candidate vertex was formed from every pair of oppositely charged tracks identified as being kaon consistent by the Čerenkov system. The pair of tracks was required to have a two-body invariant mass less than $1.1 \text{ GeV}/c^2$ and a common vertex with a confidence level greater than 1% . All ϕ candidates with K^+K^- effective masses between 1.010 and $1.030 \text{ GeV}/c^2$ were selected for the D_s lifetime analysis.

The K^+ and K^- tracks from the selected ϕ candidates were combined with each track in the event identified by the Čerenkov system as being consistent with the pion hypothesis to form the three-track D_s candidates. A standard E687 "candidate-driven" vertexing algorithm [5] was used to form primary (production) and secondary (decay) vertices.

The distinct topology of charm events (i.e., the existence of two spatially separated vertices) provides the single most powerful tool to isolate the signal from the noncharm background. The spatial separation ℓ between the reconstructed production and decay vertices divided by its error σ_ℓ is a measure of the probability of the existence of two separate vertices. Shown in Fig. 1 are the $\phi\pi$ invariant mass distributions for various lower limits on the significance of the detachment variable ℓ/σ_ℓ . The higher mass peak in these distributions corresponds to the D_s while the lower peak corresponds to the Cabibbo-suppressed decay of the D^+ .

The decay $D_s \rightarrow \phi\pi$ is the decay of a pseudoscalar state into a vector and a pseudoscalar for which the angle between one of the kaons and the pion in the rest frame of the ϕ should follow a $\cos^2\theta$ distribution. This fact was exploited to improve the signal-to-noise ratio further by requiring $|\cos\theta| > 0.3$. This requirement retained 97% of the signal while removing 30% of the background.

A detachment cut of $\ell/\sigma_\ell > 3$ was used for the final D_s lifetime measurement. A fit to the $\phi\pi$ invariant mass distribution including two Gaussian peaks for the D_s and D^+ signals and a linear background yielded $900 \pm 43 D_s$ events at a central mass $M_{D_s} = 1968.0 \pm 0.5 \text{ MeV}/c^2$ and

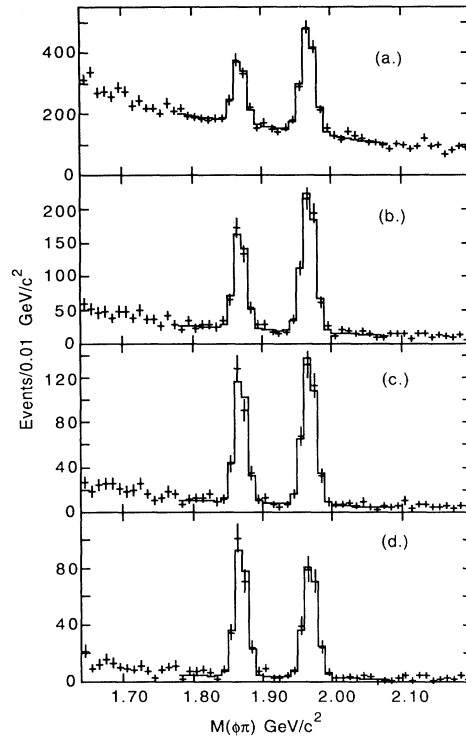


FIG. 1. Distributions of the $\phi\pi$ invariant mass for (a) $\ell/\sigma_\ell > 3$; (b) $\ell/\sigma_\ell > 8$; (c) $\ell/\sigma_\ell > 13$; and (d) $\ell/\sigma_\ell > 18$. The crosses are the data points and the histograms are the fits to the data.

a width $\sigma_{D_s} = 10.1 \pm 0.5 \text{ MeV}/c^2$ which is consistent with our resolution.

The D_s lifetime was measured using a binned maximum likelihood fitting technique [6]. A fit was made to the reduced proper time distribution. The reduced proper time t' is defined as $t' = (\ell - N\sigma_\ell)/\beta\gamma c$ where N represents the significance-of-detachment cut used, and $\beta\gamma c$ is the laboratory frame Lorentz boost of the D_s . In the absence of absorption or acceptance effects, the measured t' distribution for D_s events is expected to be of the form $\exp(-t'/\tau)$, where τ is the lifetime of the D_s , as long as σ_ℓ is independent of ℓ . (Studies of both data and Monte Carlo samples have shown that this implicit assumption is valid.)

The binned maximum likelihood method allows direct use of the proper time distribution of the data above and below the D_s mass peak to represent the background underneath the signal instead of using a background parametrization. The fit used two reduced proper time histograms: one for events which lie within the D_s mass peak ($M_{D_s} \pm 2\sigma_{D_s}$), and one for events from the combination of two sidebands representing the background. The two sidebands were chosen below (1.908 – $1.928 \text{ GeV}/c^2$) and above (2.008 – $2.028 \text{ GeV}/c^2$) the D_s mass. These histograms spanned the reduced proper time range between 0 and 3 ps in twenty bins. The observed number

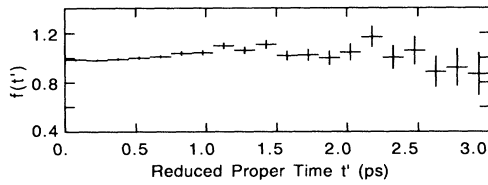


FIG. 2. The correction factor $f(t')$ to the reduced proper time as a function of reduced proper time.

of events in a reduced proper time bin i (centered at t'_i) in the signal and sideband histograms are labeled s_i and b_i , respectively. The predicted number of events n_i in a reduced proper time bin is given by

$$n_i = S \frac{f(t'_i) \exp(-t'_i/\tau)}{\sum f(t'_i) \exp(-t'_i/\tau)} + B \frac{b_i}{\sum b_i},$$

where S and B are the total number of signal and background events in the signal region and $f(t'_i)$ is a correction function. The fit parameters are B and τ while S is constrained to be the total number of signal region events minus B .

The function $f(t')$, derived from Monte Carlo simulation, corrects the proper time evolution of the signal for the effects of geometric acceptance, analysis cuts, hadronic absorption, and decay of charm secondaries. Figure 2 displays $f(t')$ as a function of t' for $\ell/\sigma_\ell > 3$. The values of $f(t')$ used in the fit were taken directly from the displayed histogram. The fitted lifetime was shown to be insensitive to the statistical fluctuations at high values of the proper time in the Monte Carlo sample.

In order to relate B to the number of background events expected from the population of the sidebands while taking into account statistical fluctuations in the background level, a factor \mathcal{L}_{bg} is included in the likelihood function. The background level is thereby jointly determined from the invariant mass distribution and from the reduced proper time evolution in the sidebands. The likelihood function is then given by

$$\mathcal{L} = \mathcal{L}_{\text{signal}} \times \mathcal{L}_{\text{bg}},$$

where

$$\mathcal{L}_{\text{signal}} = \prod_{i=1}^{\text{bins}} \frac{n_i^{s_i}}{s_i!} \exp(-n_i),$$

and

$$\mathcal{L}_{\text{bg}} = \frac{(\mu_{\text{bg}})^{N_{\text{bg}}}}{N_{\text{bg}}!} \exp(-\mu_{\text{bg}}),$$

with $N_{\text{bg}} = \sum b_i$ and $\mu_{\text{bg}} = B/R$, where R is the ratio of widths of the signal and sideband mass regions.

In order to search for possible fit biases and to verify that the errors are estimated properly, several thousand Monte Carlo replicas of our final data sample were generated. These samples were generated to be identical in

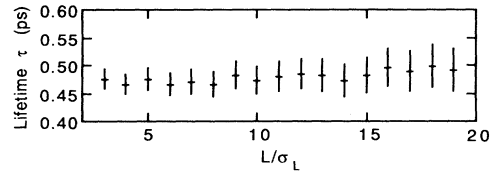


FIG. 3. The fitted lifetime as a function of the ℓ/σ_ℓ cut. The error bars shown are statistical errors only.

size to the final data sample with an exponential function being used to model the proper time evolution of the signal. The background proper time evolution was modeled by a sum of two exponential functions whose parameters were derived from the data. The distribution of the fitted lifetime from these simulated data samples revealed the presence of a small positive bias (overestimating the lifetime) of 0.002 ps, while the error calculated by the fitter proved to be accurate. All quoted lifetime values have been corrected for this bias.

In Fig. 3 the fitted lifetime is plotted versus the ℓ/σ_ℓ detachment cut used. There is no significant variation of the fitted value of the lifetime with ℓ/σ_ℓ . The final value for the lifetime from this work is chosen to be the value at $\ell/\sigma_\ell > 3$ which is in a region with a good signal-to-noise ratio and a small statistical error. The value obtained for the lifetime is $\tau_{D_s} = 0.475 \pm 0.020$ ps. The background-subtracted Monte Carlo corrected t' distribution for the D_s signal is shown in Fig. 4 along with the t' distributions of the signal and sidebands. Superimposed is a pure exponential function with the fitted value of the D_s lifetime.

The large sample of detected decays permitted a number of consistency checks and studies of systematic effects to be performed. Studies included fits using the proper time instead of the reduced proper time as the fit variable; fits using different reduced proper time bin sizes; fits using different values for the maximum reduced proper time; fits where the data were divided as to whether

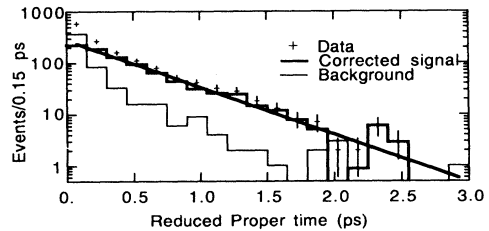


FIG. 4. The background subtracted and Monte Carlo corrected lifetime evolution of the D_s sample for $\ell/\sigma_\ell > 3$ shown as the thick-lined histogram. The crosses show the t' distribution of the events in the signal region and the thin-lined histogram shows the side band t' distribution used to represent the background. The straight line is an exponential with the fitted lifetime.

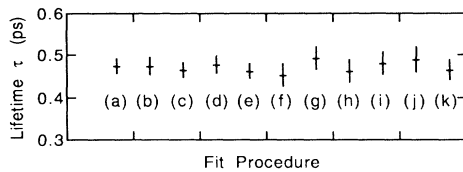


FIG. 5. A comparison of measured D_s lifetimes from different consistency checks and studies of systematic effects described in the text. The error bars shown are statistical errors only. The values are the results obtained (a) in this analysis; (b) using sideband regions 1.788–1.808 GeV/c^2 and 2.008–2.028 GeV/c^2 ; (c) using only sideband region 2.008–2.048 GeV/c^2 ; (d) eliminating events in the D^+ reflection region; (e) eliminating events in the Λ_c reflection region; (f) using only events with D_s momentum $> 95 \text{ GeV}/c$; (g) using only events with D_s momentum $< 95 \text{ GeV}/c$; (h) using D_s^+ (particle) events only; (i) using D_s^- (antiparticle) events only; (j) using upstream primary vertices only; and (k) using downstream primary vertices only.

the production vertex was in the upstream or the downstream end of the Be target; fits using different sideband regions to model the background as well as different fractions of lower and upper sidebands; fits eliminating data in kinematic regions where background due to possible reflections from other (misidentified) charm decays such as $D^\pm \rightarrow K\pi\pi$ and $\Lambda_c \rightarrow pK\pi$ could occur (based on Monte Carlo simulations, such contaminations are expected to be negligible); and fits where the data were divided into low ($p < 95 \text{ GeV}/c$) and high ($p > 95 \text{ GeV}/c$) ranges of the D_s momentum. Lifetime values from these studies for $\ell/\sigma_\ell > 3$ are shown in Fig. 5. It is evident that all the results are consistent with each other and that any systematic errors are small in comparison with the statistical error.

Systematic uncertainties in the lifetime measurement can arise due to several factors. First, an error can be made due to uncertainties in the target absorption corrections. Two effects are present: hadronic absorption of secondaries, which if not taken into account would increase the fitted lifetime; and absorption of the D_s in the target, which if ignored would tend to decrease the fitted lifetime. The systematic error arises because of the uncertainty regarding the extent to which elastic scattering of charm secondaries can cause severe mismeasurement of the parent D_s , and the fact that the D_s absorption cross section is unknown. (The kaon absorption cross section [7] was used to approximate the D_s absorption cross section.) A systematic uncertainty of 0.005 ps is attributed to the lifetime of the D_s due to the presence of these two effects.

Another source of systematic uncertainty arises because the acceptance of charm decay products depends

on the parent momentum distribution and on the transverse position of the decay vertex. D_s mesons with higher momentum tend to decay closer to the microstrips than those with lower momentum and thus have a higher acceptance. Those that decay at the outer edges of the experimental target tend to have lower acceptance than those decaying in the central region because of the finite acceptance of the microstrip system. Thus differences between the assumed D_s momentum distribution and photon beam profile and the true momentum distribution and beam profile could be a source of systematic bias. A systematic uncertainty of 0.003 ps is ascribed to these two effects.

Another source of systematic uncertainty comes from uncertainties in the background time evolution. By performing fits with different fractions of the low and high sidebands, this uncertainty is estimated to be 0.003 ps. Uncertainty in the correction function $f(t')$ due to the finite Monte Carlo statistics introduces a 0.0025 ps systematic uncertainty in the lifetime measurement. Combining all sources of systematic errors in quadrature, a total systematic uncertainty of 0.007 ps is assigned to this measurement.

In summary, a new measurement of the D_s lifetime based on a sample of 900 fully reconstructed $D_s \rightarrow \phi\pi$ decays is reported. The measured lifetime is $0.475 \pm 0.020(\text{statistical}) \pm 0.007(\text{systematic})$ ps. We conclude by noting that our result will raise the previous world average [8] and decrease its error, increasing the significance of the difference between the measured lifetimes of the D_s and the D^0 .

We wish to acknowledge the assistance of the staffs of Fermilab and the INFN of Italy, and the physics departments of our Universities. This research was supported in part by the National Science Foundation, the U.S. Department of Energy, the Italian Istituto Nazionale di Fisica Nucleare and Ministero dell'Università e della Ricerca Scientifica e Tecnologica, and the Korean Science and Engineering Foundation.

* Now at Fermilab, Batavia, IL 60510.

† Now at Dipartimento di Fisica dell'Università and INFN-Milano, I-20133 Milano, Italy.

- [1] J.R. Raab *et al.*, Phys. Rev. D **37**, 2391 (1988).
- [2] P.L. Frabetti *et al.*, Phys. Lett. B **251**, 639 (1990).
- [3] S. Barlag, *et al.*, Z. Phys. C **46**, 563–567 (1990).
- [4] H. Albrecht *et al.*, Phys. Lett. B **210**, 267 (1988).
- [5] P.L. Frabetti *et al.*, Nucl. Instrum. Methods. Phys. Res., Sect. A **320**, 519 (1992).
- [6] P.L. Frabetti *et al.*, Phys. Lett. B **263**, 584 (1991).
- [7] S.P. Denisov *et al.*, Nucl. Phys. **B61**, 62 (1973).
- [8] Particle Data Group, K. Hikasa *et al.*, Phys. Rev. D **45**, S1 (1992).